Zone Determinant Expansions for Nuclear Lattice Simulations

Dean J. Lee*

Department of Physics, North Carolina State University, Box 8202, Raleigh, NC 27695

Ilse C.F. Ipsen†

Center for Research in Scientific Computation,

North Carolina State University, Box 8205, Raleigh, NC 27695

Abstract

We discuss simulations of finite temperature nuclear matter on the lattice. We introduce a new approximation to nucleon matrix determinants that is physically motivated by chiral effective theory. The method involves breaking the lattice into spatial zones and expanding the determinant in powers of the boundary hopping parameter.

PACS numbers: 21.65.+f, 21.30.-x, 02.70.-c

Keywords: nuclear, matter, simulation, lattice, determinant, zone

*Electronic address: djlee3@unity.ncsu.edu

†Electronic address: ipsen@math.ncsu.edu

I. INTRODUCTION

We consider quantum simulations of nuclear matter on the lattice. In particular we address the problem of calculating the contribution of nucleon/nucleon-hole loops at nonzero nucleon density. With the help of auxiliary boson fields, all nucleon interactions can be written in terms of one-body interactions in a fluctuating background. In the grand canonical ensemble, the contribution of nucleon/nucleon-hole loops to the partition function equals the determinant of the one-body interaction matrix. Since the determinant of the interaction matrix for a general boson field configuration is not positive, stochastic methods such as hybrid Monte Carlo [1][2][3] do not give the sign or phase of the determinant. Instead one must rely on much slower and more memory intensive algorithms based on LU factorization.

The number of required operations in LU factorization for an $n \times n$ matrix scales as n^3. It has been shown in the literature that repeated calculations of matrix determinants with only localized changes can be streamlined in various ways [4][5]. However it is difficult to avoid the poor scaling inherent in the method. If V is the spatial volume and β is the inverse temperature measured in lattice units, a simulation that includes nucleon/nucleon-hole loops requires $(V\beta)^3$ times more operations than the corresponding quenched simulation without loops. This slowdown should not be confused with the infamous fermion sign or phase problem [27] which becomes significant at temperatures $T \leq 1$ MeV. The computational bottleneck we are considering is due to the inefficiencies of the algorithm and persists at all temperatures. It is this numerical challenge which sets current limits on nuclear lattice simulations.

In this paper we introduce a new approach to approximating nucleon matrix determinants. We begin with a review of the current status of nuclear matter simulations on the lattice and look to chiral effective theory to determine the relative importance of various interactions. We then introduce the concept of spatial zones and suggest a new expansion of the nucleon determinant in powers of the hopping parameter connecting neighboring zones. Rigorous bounds on the convergence of this expansion are given as well as an estimate of the required size of the spatial zones as a function of temperature. We apply the expansion to a realistic lattice simulation of the interactions of neutrons and neutral pions.

II. NUCLEAR LATTICE SIMULATIONS

Recently Müller, Koonin, Seki, and van Kolck [6], pioneered the study of quantum many body effects in infinite nuclear matter at finite density and temperature. In their work they considered only nucleon degrees of freedom and used an effective Hamiltonian of the form

$$H = K + V_c + V_\sigma, \tag{1}$$

where K is the kinetic energy, V_c is the two-body scalar potential, and V_σ is the two-body tensor potential. While the simulation was done on the lattice we will write their Hamiltonian in the more familiar continuum language. In the continuum K, V_c, and V_σ take the form

$$K = -\tfrac{1}{2m_N}\int d^3\vec{x}\,\psi^\dagger_{\sigma\tau}\vec{\nabla}^2\psi_{\sigma\tau}, \tag{2}$$

$$V_c = \tfrac{1}{2}\int d^3\vec{x}d^3\vec{x}'\,\psi^\dagger_{\sigma\tau}(\vec{x})\psi^\dagger_{\sigma'\tau'}(\vec{x}')V_c(\vec{x}-\vec{x}')\psi_{\sigma'\tau'}(\vec{x}')\psi_{\sigma\tau}(\vec{x}), \tag{3}$$

$$V_\sigma = \tfrac{1}{2}\int d^3\vec{x}d^3\vec{x}'\,\psi^\dagger_{\xi\tau}(\vec{x})\psi^\dagger_{\xi'\tau'}(\vec{x}')V_\sigma(\vec{x}-\vec{x}')\vec{\sigma}_{\xi\tau\kappa\lambda}\cdot\vec{\sigma}_{\xi'\tau'\kappa'\lambda'}\psi_{\kappa'\lambda'}(\vec{x}')\psi_{\kappa\lambda}(\vec{x}). \tag{4}$$

In our notation summations are implied over repeated indices. m_N is the nucleon mass. $\psi^\dagger_{\sigma\tau}(\psi_{\sigma\tau})$ creates(annihilates) a nucleon of spin σ and isospin τ, and $\vec{\sigma}_{\xi\tau\kappa\lambda}$ are the elements of a generalized Pauli spin-isospin matrix. Both potentials are assumed to have Skyrme-like on-site and next-nearest-neighbor interactions,

$$V_c(\vec{x}-\vec{x}') = V_c^{(0)}\delta(\vec{x}-\vec{x}') + V_c^{(2)}\vec{\nabla}^2\delta(\vec{x}-\vec{x}'), \tag{5}$$

$$V_\sigma(\vec{x}-\vec{x}') = V_\sigma^{(0)}\delta(\vec{x}-\vec{x}') + V_\sigma^{(2)}\vec{\nabla}^2\delta(\vec{x}-\vec{x}'). \tag{6}$$

The grand canonical partition function is given by

$$Z = Tr\left[\exp\left[-\beta\left(H-\mu_\tau n_\tau\right)\right]\right], \tag{7}$$

where μ_τ is the isospin-dependent chemical potential and n_τ is the nucleon number operator for isospin index τ. We can rewrite the quartic interactions in V_c and V_σ using the Hubbard-Stratonovich transformation [7][8]. The Hubbard-Stratonovich transformation uses the identity,

$$\exp(\tfrac{1}{2}A^2) = \sqrt{2\pi}\int_{-\infty}^{\infty} d\varphi\,\exp(-\tfrac{1}{2}\varphi^2 - \varphi A), \tag{8}$$

where A is any quantum operator. This allows the mapping of the interacting nucleon problem to a system of noninteracting nucleons coupled to a fluctuating background field. With this transformation the expectation value of any observable O can be written as

$$\langle O \rangle = \frac{\int D\phi G(\phi) \det(M(\phi)) O(\phi)}{\int D\phi G(\phi) \det(M(\phi))}, \tag{9}$$

where ϕ collectively represents the Hubbard-Stratonovich fields (as well as any other bosonic fields), $M(\phi)$ is the one-body nucleon interaction matrix, and $G(\phi)$ is a function of the ϕ's.

Using this formalism Müller, *et. al.*, were able to measure the thermodynamic properties of nuclear matter and find signs of a first order phase transition from an uncorrelated Fermi gas to a clustered phase. They examined temperatures from 3.0 MeV to 100 MeV with up to 30 time steps and a spatial volume of 4^3 with lattice spacing $a = 1.842$ fm. Unfortunately the LU factorization algorithm used to compute determinants in the simulation scales as $(V\beta)^3$ and thus going beyond lattice systems of size 4^3 is problematic.

III. CHIRAL EFFECTIVE THEORY AND NUCLEAR FORCES

There have been several recent efforts to describe nuclear forces starting from chiral effective theory. This line of study was initiated by Weinberg [9][10][11]. The idea is to expand the nuclear interactions in powers of q/Λ_χ, where q is the typical external momentum of the nucleons and Λ_χ is the chiral symmetry breaking scale or equivalently the hadronic mass scale (~ 1 GeV). The momentum cutoff scale Λ for the effective theory is set below Λ_χ, and the renormalization group flow of operator coefficients from scale Λ_χ to Λ suppress the effects of higher dimensional operators. Chiral symmetry in the limit of zero quark mass imposes additional constraints on the possible momentum and spin dependence of the interaction terms. Assuming naturalness for the renormalized coupling constants in the Lagrangian at the scale Λ_χ, one expects in the low energy effective theory that contributions to nucleon forces from operators at higher order in the chiral expansion to be negligible.

Weinberg's work was followed by applications of chiral effective theory to the nucleon potential [12] and alternative approaches to power counting without apparent fine tuning in the presence of long scattering lengths [13][14]. Recent low energy studies [15][16][17][18] have also integrated out pion fields to produce energy independent two- and three- nucleon potentials, and the effective theory approach has been used to calculate nuclear spectra as

well as phase shifts and scattering lengths which compare favorably with potential model calculations.

In Weinberg's power counting scheme one deals with infrared singularities in bound state problems by distinguishing between reducible and irreducible diagrams. Reducible diagrams are those that can be disconnected by cutting internal lines that correspond with particles in the initial or final state. In the notation of [12], the power of q/Λ_χ for any irreducible or non-reducible diagram is given by

$$\nu = 4 - \tfrac{E_f}{2} + 2L - 2C + \sum_i V_i \delta_i, \tag{10}$$

where E_f is the number of external nucleon lines, L is the number of loops, C is the number of connected pieces, V_i is the number of vertices of type i, and δ_i is the index of vertex i. The index δ_i is given by

$$\delta_i = d_i + \tfrac{f_i}{2} - 2, \tag{11}$$

where d_i is the number of derivatives and f_i is the number of nucleon fields in the vertex.

We let N represent the nucleon fields,

$$N = \begin{bmatrix} p \\ n \end{bmatrix} \otimes \begin{bmatrix} \uparrow \\ \downarrow \end{bmatrix}. \tag{12}$$

We use τ_i to represent Pauli matrices acting in isospin space, and we use $\vec{\sigma}$ to represent Pauli matrices acting in spin space. Pion fields are notated as π_i, and μ is the nucleon chemical potential. We denote the pion decay constant as $F_\pi \approx 183$ MeV and let

$$D = 1 + \pi_i^2/F_\pi^2. \tag{13}$$

The lowest order Lagrange density for low energy pions and nucleons is given by terms with $\delta_i = 0$,

$$\begin{aligned} \mathcal{L}^{(0)} = & -\tfrac{1}{2} D^{-2} \left[(\vec{\nabla}\pi_i)^2 - \dot{\pi}_i^2 \right] - \tfrac{1}{2} D^{-1} m_\pi^2 \pi_i^2 + \bar{N}[i\partial_0 - (m_N - \mu)]N \\ & - D^{-1} F_\pi^{-1} g_A \bar{N} \left[\tau_i \vec{\sigma} \cdot \vec{\nabla}\pi_i \right] N - D^{-1} F_\pi^{-2} \bar{N}[\epsilon_{ijk} \tau_i \pi_j \dot{\pi}_k] N \\ & - \tfrac{1}{2} C_S \bar{N} N \bar{N} N - \tfrac{1}{2} C_T \bar{N} \vec{\sigma} N \cdot \bar{N} \vec{\sigma} N. \end{aligned} \tag{14}$$

g_A is the nucleon axial coupling constant, and ϵ_{ijk} is the Levi-Civita symbol. For the purposes of power counting, the pion mass m_π is equivalent to one power of the momentum q. The

nucleon mass term $\bar{N}N$ actually has index $\delta_i = -1$. However the coefficient of this term is fine-tuned using μ to set the nucleon density, and so the $\bar{N}N$ term is reduced to the same size as other terms with index $\delta_i = 0$. At next order we have terms with $\delta_i = 1$,

$$\mathcal{L}^{(1)} = \tfrac{1}{2m_N} \bar{N} \vec{\nabla}^2 N + ... \tag{15}$$

The important point for our discussion is that the lowest order Lagrange density $\mathcal{L}^{(0)}$ describes static nucleons. Spatial hopping of nucleons first appears at subleading index $\delta_i = 1$. This suggests that in some cases one could compute the determinant of the nucleon interaction matrix as an expansion in powers of the spatial hopping parameter. We should note one point of caution though. The $\mathcal{L}^{(1)}$ kinetic energy term cannot be ignored if the infrared singularities of $\mathcal{L}^{(0)}$ are not properly dealt with. Since diagrammatic methods are not used in nuclear matter Monte Carlo simulations, we cannot separate reducible and irreducible diagrams. However if the simulation is done at non-zero temperature T then that will serve to regulate the infrared singularities. We will explicitly see the effect of temperature on the convergence of the expansion later in our discussion.

IV. SPATIAL ZONES

In [19] spatial zones were used to calculate the chiral condensate for massless QED$_3$. In that paper the main problem was dealing with sign and phase problems that arise in the Hamiltonian worldline formalism with explicit fermions. The idea of the zone method is that fermions at inverse temperature β with spatial hopping parameter h have a localization length of

$$l \sim \sqrt{\beta h}. \tag{16}$$

We now apply the zone idea to our determinant problem. Let M be the nucleon matrix, in general an $n \times n$ complex matrix. We partition the lattice spatially into separate zones such that the length of each zone is much larger than the localization length l. Since most nucleon worldlines do not cross the zone boundaries, they would not be affected if we set the zone boundary hopping terms to zero. Hence we anticipate that the determinant of M can be approximated by the product of the submatrix determinants for each spatial zone.

Let us partition the lattice into spatial zones labelled by index j. Let $\{P_j\}$ be a complete set of matrix projection operators that project onto the lattice sites within spatial zone j.

We can write

$$M = \sum_{i,j} P_j M P_i = M_0 + M_E, \tag{17}$$

where

$$M_0 = \sum_i P_i M P_i, \tag{18}$$

$$M_E = \sum_{i \neq j} P_j M P_i. \tag{19}$$

If the zones can be sorted into even and odd sets so that

$$P_j M P_i = 0 \tag{20}$$

whenever i is even and j is odd or vice-versa, then we say that the zone partitioning is bipartite. We now have

$$\begin{aligned} \det(M) &= \det(M_0) \det(1 + M_0^{-1} M_E) \\ &= \det(M_0) \exp(\mathrm{trace}(\log(1 + M_0^{-1} M_E))). \end{aligned} \tag{21}$$

Using an expansion for the logarithm, we have

$$\det(M) = \det(M_0) \exp\left(\sum_{p=1}^{\infty} \frac{(-1)^{p-1}}{p} \mathrm{trace}((M_0^{-1} M_E)^p) \right). \tag{22}$$

Let us define

$$\Delta_m = \det(M_0) \exp\left(\sum_{p=1}^{m} \frac{(-1)^{p-1}}{p} \mathrm{trace}((M_0^{-1} M_E)^p) \right). \tag{23}$$

Let $\lambda_k(M_0^{-1} M_E)$ be the eigenvalues of $M_0^{-1} M_E$ and R be the spectral radius,

$$R = \max_{k=1,\ldots,n} (\left| \lambda_k(M_0^{-1} M_E) \right|). \tag{24}$$

It has been shown [20] that for $R < 1$

$$\frac{|\det(M) - \Delta_m|}{|\Delta_m|} \leq c R^m e^{c R^m} \tag{25}$$

where

$$c = -n \log(1 - R). \tag{26}$$

The spectral radius R determines the convergence of our expansion. R can be reduced by increasing the size of the spatial zone relative to the localization length l. In the special case where the zone partitioning is bipartite, we note that for any odd p,

$$\mathrm{trace}((M_0^{-1}M_E)^p) = 0. \tag{27}$$

In that case

$$\Delta_{2m+1} = \Delta_{2m}, \tag{28}$$

and so we gain an extra order of accuracy without additional work.

V. APPLICATION TO NEUTRON MATTER SIMULATIONS

We now illustrate the zone determinant expansion for a simple but realistic lattice simulation of neutron matter. The formalism we use is a merger of chiral effective theory and Euclidean lattice methods. A full account of this new approach will be given elsewhere [21].

Our starting point is the same as that of Weinberg [9]. We start with the most general local Lagrange density involving pions and low-energy nucleons consistent with Lorentz and translational invariance, isospin symmetry, and spontaneously broken chiral symmetry. This will produce an infinite set of interaction terms with increasing numbers of derivatives and/or nucleon fields. The dependence of each term on the pion field is governed by the rules of spontaneously broken chiral symmetry. Degrees of freedom associated with heavier mesons such as the ρ, heavier baryons such as the Δ's as well as antinucleons are all integrated out. We also integrate out nucleons with momenta greater than the cutoff scale Λ. The contribution of these effects appear as coefficients of local terms in our pion-nucleon Lagrangian.

For simplicity we consider only neutrons and neutral pions. We let ψ represent the neutron spin states,

$$\psi = \begin{bmatrix} \uparrow \\ \downarrow \end{bmatrix}. \tag{29}$$

The terms in our effective pion-nucleon Euclidean action are

$$S = S_{\pi\pi} + S_{\bar{N}N} + S_{\pi\bar{N}N} + S_{\bar{N}N\bar{N}N}, \tag{30}$$

where

$$S_{\pi\pi} = \int d^3\vec{r}dr_4 \left[\tfrac{1}{2}(\tfrac{\partial\pi_0}{\partial r_4})^2 + \tfrac{1}{2}(\vec{\nabla}\pi_0)^2 + \tfrac{1}{2}m_\pi^2\pi_0^2\right], \tag{31}$$

$$S_{\bar{N}N} = \int d^3\vec{r}dr_4 \left[\psi^\dagger\tfrac{\partial\psi}{\partial r_4} - \psi^\dagger\tfrac{\vec{\nabla}^2\psi}{2m_N} + (m_N-\mu)\psi^\dagger\psi\right], \tag{32}$$

$$S_{\pi\bar{N}N} = \int d^3\vec{r}dr_4 \left[-g\psi^\dagger\left(\vec{\sigma}\cdot\vec{\nabla}\pi_0\right)\psi\right], \tag{33}$$

$$S_{\bar{N}N\bar{N}N} = \int d^3\vec{r}dr_4 \left[\tfrac{1}{2}C{:}\psi^\dagger\psi\psi^\dagger\psi{:}\right]. \tag{34}$$

We have kept terms in the lowest order chiral Lagrange density $\mathcal{L}^{(0)}$ containing neutrons and neutral pions. We have dropped the factors of D^{-1} which at lowest order contribute to multipion processes. We have also chosen to include the neutron kinetic energy term even though it appears in $\mathcal{L}^{(1)}$. This is useful if we wish to recover the exact free neutron Fermi gas in the weak coupling limit.

On the lattice we let a be the spatial lattice spacing and a_t be the temporal lattice spacing. We use the notation $\hat{1}, \hat{2}, \hat{3}$, or $\hat{4}$ to represent vectors that extend exactly one lattice unit (either a or a_t) in the respective direction. We use dimensionless lattice fields and dimensionless masses and couplings by multiplying by the corresponding power of a. For example,

$$\hat{m}_\pi = m_\pi \cdot a \tag{35}$$

$$\hat{m}_N = m_N \cdot a \tag{36}$$

$$\hat{g} = g \cdot a^{-1} \tag{37}$$

$$\hat{\mu} = \mu \cdot a \tag{38}$$

$$\hat{C} = C \cdot a^{-2}. \tag{39}$$

We use standard fermion path integral conventions at finite time step [22][23] and define

$$\psi'(\vec{n}) = \psi(\vec{n} - \hat{4}) \tag{40}$$

in order to write the lattice path integral in standard form. The lattice actions have the form

$$\begin{aligned} S_{\pi\pi} = &-\tfrac{a}{a_t}\sum_{\vec{n}}\pi(\vec{n})\pi(\vec{n}+\hat{4}) - \tfrac{a_t}{a}\sum_{\vec{n},l=1,2,3}\pi(\vec{n})\pi(\vec{n}+\hat{l}) \\ &+ ((\tfrac{\hat{m}_\pi^2}{2}+3)\tfrac{a_t}{a} + \tfrac{a}{a_t})\sum_{\vec{n}}(\pi(\vec{n}))^2, \end{aligned} \tag{41}$$

$$S_{\bar{N}N} = \sum_{\vec{n}} \psi^\dagger(\vec{n})\psi'(\vec{n}+\hat{4}) - \tfrac{a_t}{2\hat{m}_N a} \sum_{\vec{n},l=1,2,3} (\psi^\dagger(\vec{n})\psi'(\vec{n}+\hat{l}) + \psi^\dagger(\vec{n})\psi'(\vec{n}-\hat{l}))$$
$$+ (-1 + (\hat{m}_N + \tfrac{3}{\hat{m}_N})\tfrac{a_t}{a} - \hat{\mu}\tfrac{a_t}{a}) \sum_{\vec{n}} \psi^\dagger(\vec{n})\psi'(\vec{n}), \tag{42}$$

$$S_{\pi\bar{N}N} = -\tfrac{\hat{g}a_t}{2a} \sum_{\vec{n}} \left[\left[\psi^*_\uparrow(\vec{n})\psi'_\uparrow(\vec{n}) - \psi^\dagger_\downarrow(\vec{n})\psi'_\downarrow(\vec{n}) \right] \left[\pi(\vec{n}+\hat{3}) - \pi(\vec{n}-\hat{3}) \right] \right]$$
$$- \tfrac{\hat{g}a_t}{2a} \sum_{\vec{n}} \left[\psi^*_\uparrow(\vec{n})\psi'_\downarrow(\vec{n}) \left[\pi(\vec{n}+\hat{1}) - \pi(\vec{n}-\hat{1}) - i\pi(\vec{n}+\hat{2}) + i\pi(\vec{n}-\hat{2}) \right] \right]$$
$$- \tfrac{\hat{g}a_t}{2a} \sum_{\vec{n}} \left[\psi^*_\downarrow(\vec{n})\psi'_\uparrow(\vec{n}) \left[\pi(\vec{n}+\hat{1}) - \pi(\vec{n}-\hat{1}) + i\pi(\vec{n}+\hat{2}) - i\pi(\vec{n}-\hat{2}) \right] \right], \tag{43}$$

$$S_{\bar{N}N\bar{N}N} = \tfrac{\hat{C}a_t}{a} \sum_{\vec{n}} \psi^*_\uparrow(\vec{n})\psi'_\uparrow(\vec{n})\psi^*_\downarrow(\vec{n})\psi'_\downarrow(\vec{n}). \tag{44}$$

We can reexpress $S_{\bar{N}N\bar{N}N}$ using a discrete Hubbard-Stratonovich transformation [24] for $\hat{C} \leq 0$,

$$\exp(-\tfrac{\hat{C}a_t}{a}\psi^*_\uparrow(\vec{n})\psi'_\uparrow(\vec{n})\psi^*_\downarrow(\vec{n})\psi'_\downarrow(\vec{n}))$$
$$= \tfrac{1}{2} \sum_{s=\pm 1} \exp\left[-(\tfrac{\hat{C}a_t}{2a} + \lambda s)(\psi^*_\uparrow(\vec{n})\psi'_\uparrow(\vec{n}) + \psi^*_\downarrow(\vec{n})\psi'_\downarrow(\vec{n}) - 1) \right], \tag{45}$$

where λ is defined by

$$\cosh\lambda = \exp(-\tfrac{\hat{C}a_t}{2a}). \tag{46}$$

VI. RESULTS

For the simulation results presented in this section we use the values

$$a^{-1} = 150 \text{ MeV}, \tag{47}$$
$$a_t^{-1} = 225 \text{ MeV}, \tag{48}$$
$$C = -4.0 \cdot 10^{-5} \text{ MeV}^{-2}, \tag{49}$$
$$g = 6.8 \cdot 10^{-3} \text{ MeV}^{-1}. \tag{50}$$

The value of g is set according to the tree level Goldberger-Treiman relation [25]

$$g = F_\pi^{-1} g_A = 6.8 \cdot 10^{-3} \text{ MeV}^{-1}. \tag{51}$$

The value of C is tuned to match the s-wave phase shifts on the lattice for nucleon scattering at lattice spacing $(150 \text{ MeV})^{-1}$. The calculation of phase shifts on the lattice is discussed in a forthcoming article which details the entire formalism [21].

We present data for three independent pion and Hubbard-Stratonovich field configurations on a $4^3 \times 6$ lattice at temperature $T = 37.5$ MeV and neutron density $\rho = 0.57\rho_{\rm nucl}$ where nuclear density is

$$\rho_{\rm nucl} = 2.8 \cdot 10^{14}\ {\rm g/cm}^3 = 1.2 \cdot 10^9\ {\rm MeV}^4. \tag{52}$$

The same chemical potential is used for all simulation results presented here. We refer to spatial zones according to their x, y, z lattice dimensions $[n_x, n_y, n_z]$. At this lattice spacing and temperature our localization length estimate is

$$l \sim \sqrt{\beta h} = 0.57, \tag{53}$$

and so we expect the zone determinant expansion to converge for even the smallest zones, $[n_x, n_y, n_z] = [1, 1, 1]$, consisting of groups of lattice points with the same spatial coordinate. In Table 1 we show the spectral radius R of $M_0^{-1} M_E$ and the determinant expansion for $[1, 1, 1]$ zones for three independent pion and Hubbard-Stratonovich configurations at equilibrium.

configuration	#1	#2	#3
R	0.538	0.523	0.534
$\log(\det(M))$	$16.4727 + 0.3666i$	$18.1193 + 0.4479i$	$18.2612 - 0.1811i$
$\log(\Delta_0)$	$12.1700 + 0.3807i$	$13.7933 + 0.4900i$	$14.0060 - 0.2075i$
$\log(\Delta_2)$	$16.4964 + 0.3686i$	$18.1792 + 0.4477i$	$18.2841 - 0.1801i$
$\log(\Delta_4)$	$16.4959 + 0.3659i$	$18.1329 + 0.4468i$	$18.2856 - 0.1805i$
$\log(\Delta_6)$	$16.4664 + 0.3667i$	$18.1147 + 0.4482i$	$18.2548 - 0.1813i$
$\log(\Delta_8)$	$16.4739 + 0.3666i$	$18.1203 + 0.4478i$	$18.2622 - 0.1810i$

Table 1: Convergence of determinant series for $[1, 1, 1]$ zones

We see that the spectral radius R is less than 1 as expected from the localization length estimate. We also find that the rigorous bounds in (25) are satisfied. Since most of the eigenvalues of $M_0^{-1} M_E$ are much smaller in magnitude than the spectral radius R, we observe that the prefactor c in (25) is actually much larger than needed for these examples. From the data in Table 1 we find empirically

$$\frac{|\det(M) - \Delta_{2m}|}{|\Delta_{2m}|} = \frac{|\det(M) - \Delta_{2m+1}|}{|\Delta_{2m+1}|} \sim R^{2m+1}. \tag{54}$$

As the temperature decreases, the localization length increases and therefore the convergence of the zone determinant expansion slows down. In Table 2 we show the expansion for a $6^3 \times 6$ lattice at $T = 37.5$ MeV, $6^3 \times 9$ lattice at $T = 25.0$ MeV, and $6^3 \times 12$ lattice at $T = 18.8$ MeV.

T	37.5 MeV	25.0 MeV	18.8 MeV
R	0.5122	0.6742	0.7631
$\log(\det(M))$	$65.8009 - 0.7250i$	$37.6912 - 1.5930i$	$16.0023 + 0.0541i$
$\log(\Delta_0)$	$51.3988 - 0.7888i$	$20.7653 - 1.5752i$	$4.1999 + 0.2033i$
$\log(\Delta_2)$	$66.0028 - 0.7218i$	$36.2570 - 1.6535i$	$11.7590 + 0.0861i$
$\log(\Delta_4)$	$65.8289 - 0.7243i$	$38.0872 - 1.5800i$	$15.9390 + 0.0337i$
$\log(\Delta_6)$	$65.7926 - 0.7253i$	$37.6528 - 1.5924i$	$16.3121 + 0.0478i$
$\log(\Delta_8)$	$65.8026 - 0.7249i$	$37.6780 - 1.5943i$	$16.0111 + 0.0575i$

Table 2: Determinant series for $[1, 1, 1]$ zones for varying temperatures

The increase in R and the slowdown in the series convergence is consistent with our intuition based on the localization length. The localization length becomes greater than 1 for $T \sim 10$ MeV and we expect the series to break down for $[1, 1, 1]$ zones at colder temperatures.

On the other hand we can accelerate the convergence by using larger spatial zones. In Table 3 we show the determinant expansion for a $6^3 \times 6$ lattice at $T = 37.5$ MeV for $[1, 1, 1]$, $[2, 2, 2]$, and $[3, 3, 3]$ zones [28].

zone	$[1, 1, 1]$	$[2, 2, 2]$	$[3, 3, 3]$
R	0.5122	0.3013	0.3014
$\log(\det(M))$	$65.8009 - 0.7250i$	$65.8009 - 0.7250i$	$65.8009 - 0.7250i$
$\log(\Delta_0)$	$51.3988 - 0.7888i$	$58.6585 - 0.7543i$	$61.0471 - 0.7722i$
$\log(\Delta_2)$	$66.0028 - 0.7218i$	$65.8570 - 0.7231i$	$65.8317 - 0.7233i$
$\log(\Delta_4)$	$65.8289 - 0.7243i$	$65.8015 - 0.7251i$	$65.8007 - 0.7250i$
$\log(\Delta_6)$	$65.7926 - 0.7253i$	$65.8009 - 0.7250i$	$65.8009 - 0.7250i$
$\log(\Delta_8)$	$65.8026 - 0.7249i$	$65.8009 - 0.7250i$	$65.8009 - 0.7250i$

Table 3: Determinant series for various zone sizes

It is somewhat unusual that the spectral radius R is about the same for $[2,2,2]$ and $[3,3,3]$, however the convergence of the series clearly improves as we increase the zone size.

We now investigate the convergence of the determinant zone expansion for physical observables. Let us return to the data in Table 1 for a moment. We observe that at any given order the error appears to be about the same for each of the three independent configurations. Since the measurement of a physical observable does not dependent on the overall normalization of the partition function, this suggests that the zone determinant expansion could be more accurate in approximating physical observables. We now check to see if this is so for a particular example.

Let us define the neutron occupation number at site $\vec{r}$,

$$\rho_{\uparrow(\downarrow)}(\vec{r}) = \psi^*_{\uparrow(\downarrow)}(\vec{r})\psi_{\uparrow(\downarrow)}(\vec{r}) = \psi^*_{\uparrow(\downarrow)}(\vec{r})\psi'_{\uparrow(\downarrow)}(\vec{r}+\hat{4}). \tag{55}$$

We measure the opposite spin radial distribution function,

$$< \rho_\uparrow(\vec{r})\rho_\downarrow(0) >, \tag{56}$$

by sampling 20 independent pion and Hubbard-Stratonovich field configurations. For $r_x = 0$ we plot the results for the opposite spin radial distribution function in Fig. 1 using exact matrix determinants for a $4^3 \times 6$ lattice at $T = 37.5$ MeV. In Figs. 2-6 we show the error in the radial distribution function if the estimate Δ_m is used in place of $\det(M)$ for $m = 0, 2, 4, 6, 8$.

The approximation at order 0 is a lot better than expected given the error of Δ_0 in approximating $\det(M)$. Overall we find that the zone expansion is significantly more accurate for the radial distribution function than the expansion of the determinants. It is premature to say if this is typical of all physical observable measurements. Nevertheless if most of the error of Δ_m is in fact independent of the pion and Hubbard-Stratonovich configurations at equilibrium, then we expect an improvement in accuracy for most physical observables.

VII. SUMMARY AND CONCLUSIONS

We have discussed lattice simulations of finite temperature nuclear matter and a new approximation method called the zone determinant expansion for nucleon matrix determinants. The expansion is made possible by the small size of the spatial hopping parameter.

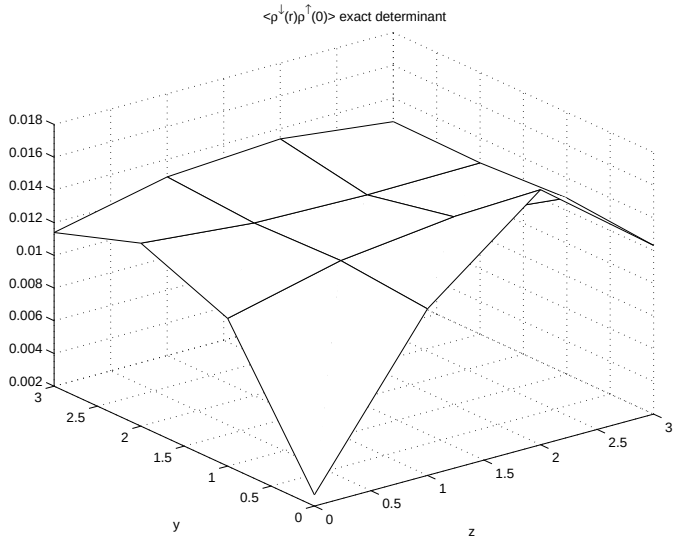

FIG. 1: Opposite spin radial distribution function using exact determinants.

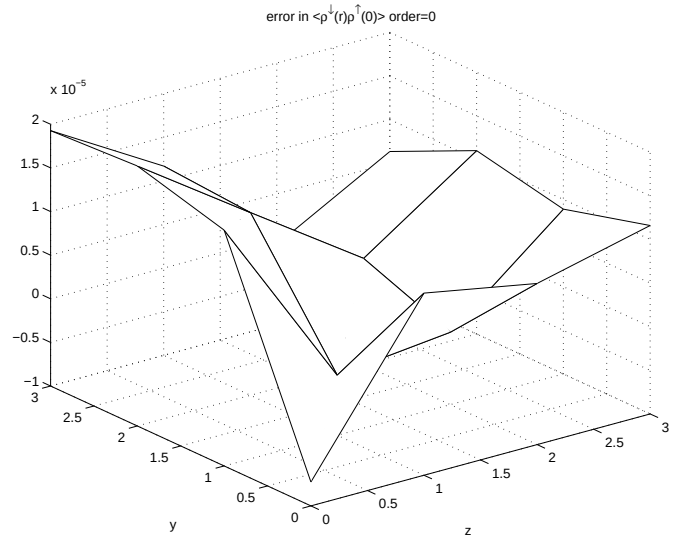

FIG. 2: Error in the opposite spin radial distribution function at order $m = 0$.

We know from power counting in chiral effective theory that the spatial hopping parameter is suppressed relative to the leading order interactions at low energies. The zone determinant expansion is given by

$$\det(M) = \det(M_0) \exp\left(\sum_{p=1}^{\infty} \frac{(-1)^{p-1}}{p} \mathrm{trace}((M_0^{-1} M_E)^p) \right), \tag{57}$$

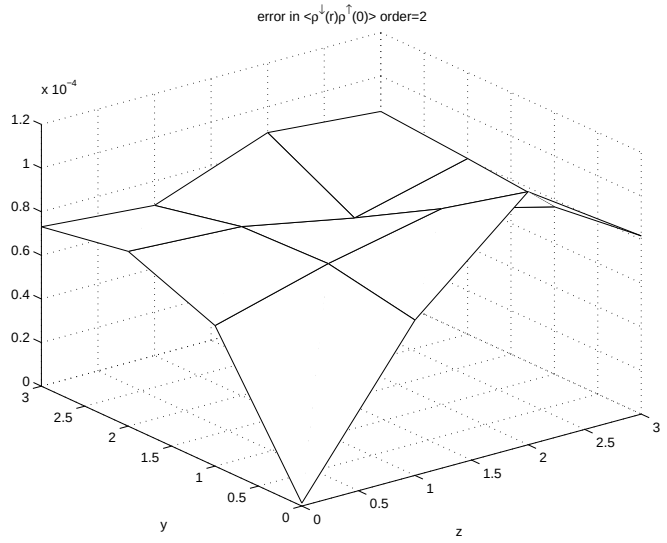

FIG. 3: Error in the opposite spin radial distribution function at order $m = 2$.

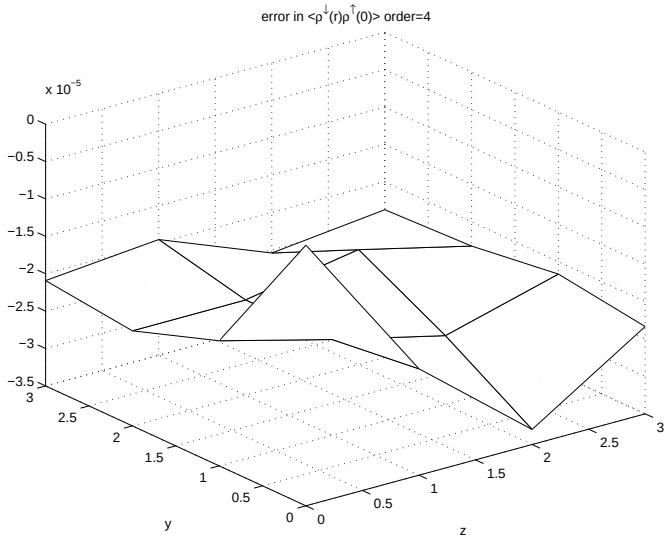

FIG. 4: Error in the opposite spin radial distribution function at order $m = 4$.

where M is the nucleon one-body interaction matrix, M_E is the submatrix consisting of zone boundary hopping terms, and M_0 is the submatrix without boundary hopping terms. The convergence of the expansion is controlled by the spectral radius of $M_0^{-1} M_E$. Physically we expect the convergence to be rapid if the localization length of the nucleons

$$l \sim \sqrt{\beta h} \tag{58}$$

is small compared to the size of the spatial zones.

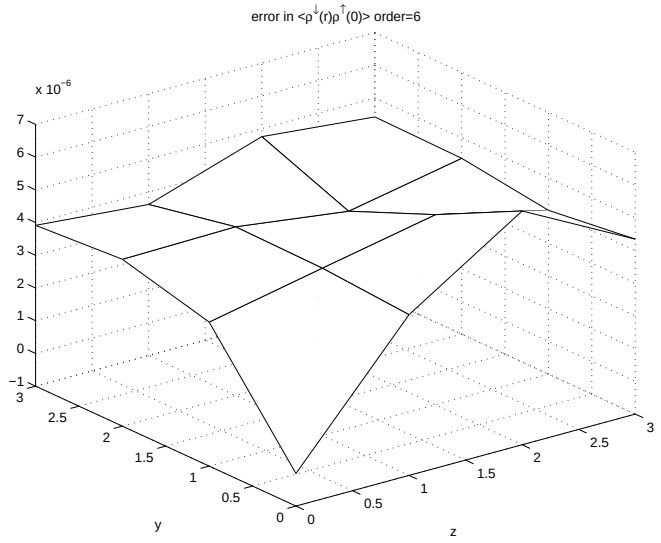

FIG. 5: Error in the opposite spin radial distribution function at order $m = 6$.

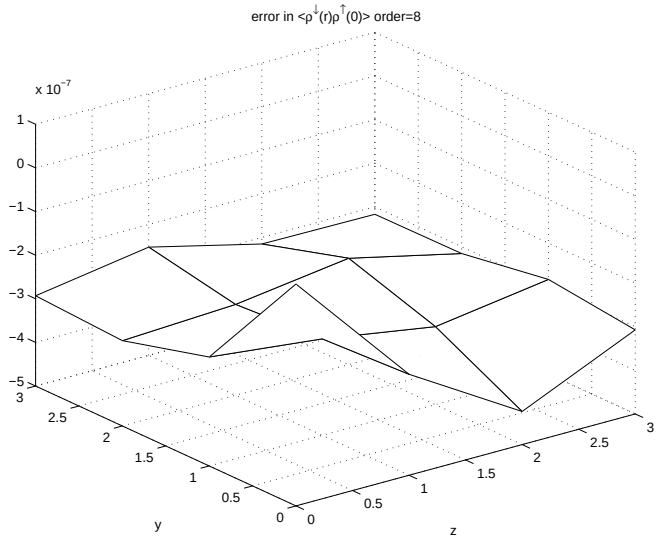

FIG. 6: Error in the opposite spin radial distribution function at order $m = 8$.

We tested the zone determinant expansion using lattice simulations of neutron matter with self interactions and neutral pion exchange. The convergence of the expansion was measured for several configurations at temperature $T = 37.5$ MeV and using $[1, 1, 1]$ spatial zones. By decreasing the temperature from $T = 37.5$ MeV to 18.8 MeV we found that the convergence of the expansion becomes slower, as predicted by the increase in the localization length. But we then showed that convergence could be accelerated by increasing the size

of the zones from $[1,1,1]$ to $[3,3,3]$. Finally we looked at the convergence of the expansion for the opposite spin radial distribution function

$$< \rho_\uparrow(\vec{r})\rho_\downarrow(0) > . \tag{59}$$

We found that the accuracy of the expansion for this physical observable was signficantly better at each order than that for the expansion of the determinants.

The number of required operations for calculating the nucleon determinant using LU factorization for an $n \times n$ matrix scales as n^3. Therefore a nuclear lattice simulation that includes nucleon/nucleon-hole loops requires $(V\beta)^3$ times more operations than the quenched simulation without loops. This numerical challenge has been the most pressing limitation on finite temperature nuclear lattice simulations to date.

For the zone determinant expansion method at fixed zone size, the computation cost scales only as $f(m)\beta^3$ where m is the order of the expansion. For a simulation on a lattice with spatial dimensions 8^3, one can accelerate the simulation by a factor of about 10^5 to 10^7, depending on the expansion order and size of the spatial zone. The savings are greater on larger lattices and should facilitate future work in the area of finite temperature nuclear lattice simulations.

Acknowledgments

D.L. is grateful to B. Borasoy, T. Schaefer, R. Seki, U. van Kolck, and participants at the 2003 CECAM Sign Problem Workshop for discussions and comments. This work is supported in part by NSF grants DMS-0209931 and DMS-0209695.

---

[1] R. T. Scalettar, D. J. Scalapino, and R. L. Sugar, Phys. Rev. **B34**, 7911 (1986).

[2] S. Gottlieb, W. Liu, D. Toussaint, R. L. Renken, and R. L. Sugar, Phys. Rev. **D35**, 2531 (1987).

[3] S. Duane, A. D. Kennedy, B. J. Pendleton, and D. Roweth, Phys. Lett. **B195**, 216 (1987).

[4] D. J. Scalapino and R. L. Sugar, Phys. Rev. Lett. **46**, 519 (1981).

[5] E. Y. J. Loh and J. E. Gubernatis, *Electronic Phase Transitions* (Elsevier Science Publishers, 1992), chap. 4, pp. 177–235.

[6] H. M. Muller, S. E. Koonin, R. Seki, and U. van Kolck, Phys. Rev. **C61**, 044320 (2000), nucl-th/9910038.

[7] R. L. Stratonovich, Soviet Phys. Doklady **2**, 416 (1958).

[8] J. Hubbard, Phys. Rev. Lett. **3**, 77 (1959).

[9] S. Weinberg, Phys. Lett. **B251**, 288 (1990).

[10] S. Weinberg, Nucl. Phys. **B363**, 3 (1991).

[11] S. Weinberg, Phys. Lett. **B295**, 114 (1992), hep-ph/9209257.

[12] C. Ordonez, L. Ray, and U. van Kolck, Phys. Rev. **C53**, 2086 (1996), hep-ph/9511380.

[13] D. B. Kaplan, M. J. Savage, and M. B. Wise, Phys. Lett. **B424**, 390 (1998), nucl-th/9801034.

[14] D. B. Kaplan, M. J. Savage, and M. B. Wise, Nucl. Phys. **B534**, 329 (1998), nucl-th/9802075.

[15] E. Epelbaum, W. Glockle, A. Kruger, and U.-G. Meissner, Nucl. Phys. **A645**, 413 (1999), nucl-th/9809084.

[16] E. Epelbaum, W. Glockle, and U.-G. Meissner, Phys. Lett. **B439**, 1 (1998), nucl-th/9804005.

[17] E. Epelbaum, W. Glockle, and U.-G. Meissner, Nucl. Phys. **A637**, 107 (1998), nucl-th/9801064.

[18] E. Epelbaum *et al.*, Phys. Rev. **C66**, 064001 (2002), nucl-th/0208023.

[19] D. Lee and P. Maris, Phys. Rev. **D67**, 076002 (2003).

[20] I. C. Ipsen and D. Lee, Determinant approximations, Submitted for publication, 2003.

[21] B. Borasoy, D. Lee, and T. Schaefer, Work in progress, 2003.

[22] D. E. Soper, Phys. Rev. **D18**, 4590 (1978).

[23] H. J. Rothe, World Sci. Lect. Notes Phys. **59**, 1 (1997).

[24] J. E. Hirsch, Phys. Rev. **B28**, 4059 (1983).

[25] M. L. Goldberger and S. B. Treiman, Phys. Rev. **111**, 354 (1958).

[26] S. Chandrasekharan, M. Pepe, F. D. Steffen, and U. J. Wiese, (2003), hep-lat/0306020.

[27] We should mention recent work [26] that shows in the chiral limit with static nucleons the sign problem does not occur. Thus there is some indirect relationship between the two problems.

[28] For $[2,2,2]$ the zone breakup is no longer biparitite since the $6 \div 2$ is odd. However this is only a boundary effect and we find that Δ_{2m+1} is extremely close to Δ_{2m}.